

### 2.1 Introduction

The X-ray absorption spectrum of any material around the absorption edge of any of its constituent atoms exhibits a series of oscillatory fine features that modulate the monotonically decreasing atomic absorption coefficient  $\mu_0$  by a few percent. This is known as X-ray absorption fine structure (XAFS).<sup>46</sup> XAFS has been attributed to the presence of other atoms around the excited atom. By analyzing XAFS, detailed structural information about the “local” environment of the absorbing atom can be derived.

Fig. 2.1 shows a typical XAFS spectrum (Au L3 edge, 11,919 eV). The spectrum can be divided into two main regions: X-ray Absorption Near Edge Structure (XANES) and Extended X-ray Absorption Fine Structure (EXAFS). XANES refers to the region close to the absorption edge ( $\leq 30\text{eV}$ ) and contains information about the chemical state (oxidation state, site symmetry, etc.) of the absorbing atom. EXAFS refers to the oscillations well above the edge ( $> 30\text{eV}$ ) and contains local structural information (near neighbor coordination number, bond lengths, Debye Waller Factors). The only real distinction between the physics of XANES and EXAFS is in terms of resolution and in the complexity of the spectra. The most important strength of XAFS is the ability to simultaneously measure chemical state and local structure. XAFS has wide ranged applications in several fields ranging from basic physics/chemistry/biology to catalysis, environmental science, device physics, optoelectronics etc.

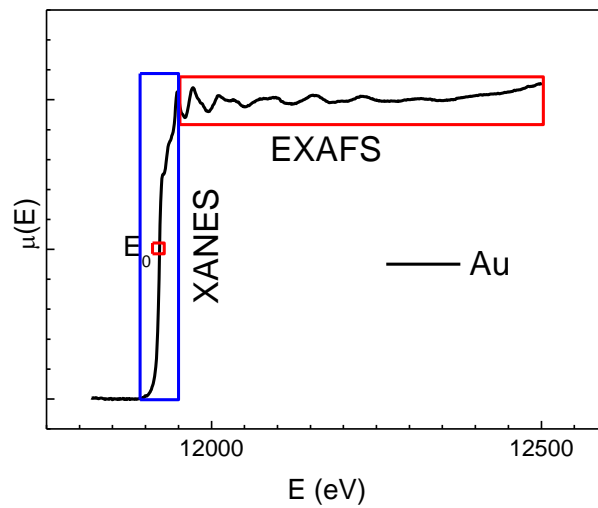


Fig. 2.1: Typical XAFS spectrum

## 2.2 Physics of XAFS

When an atom absorbs an x-ray of energy  $E \cong E_0$ , where  $E_0$  is the binding energy, a photo-electron with energy  $(E - E_0)$  is ejected (Fig. 2.2). If the x-ray energy is large enough to promote a core-level electron to the continuum, there is a sharp increase in absorption. For an isolated atom,  $\mu(E)$  resembles typical resonance spectrum i.e. rises sharply at and then monotonically drops with increasing energy (Fig. 2.3(a)). Quantum mechanically, this is due to the fact that the probability of the photon being absorbed by the electron depends on the initial and the final state of the electron, which includes the superposition of the outgoing and all incoming, backscattered waves and the potential energy difference between the atomic state and the Fermi energy. In real material, one observes oscillatory features superimposed on the mean background. The origin of these oscillations could be understood considering wave-form of the ejected photo-electron and scattering phenomenon. In real material, atoms are not isolated but surrounded by neighboring atoms. The ejected photo-electron wave back-scatters from neighboring atoms (Fig. 2.3 (b)) and interferes with itself. Thus, the final state electron wave-function is not decaying anymore; instead it is oscillatory as function of energy. The oscillations of the final electron wave are reflected as oscillations in  $\mu(E)$ , called XAFS.

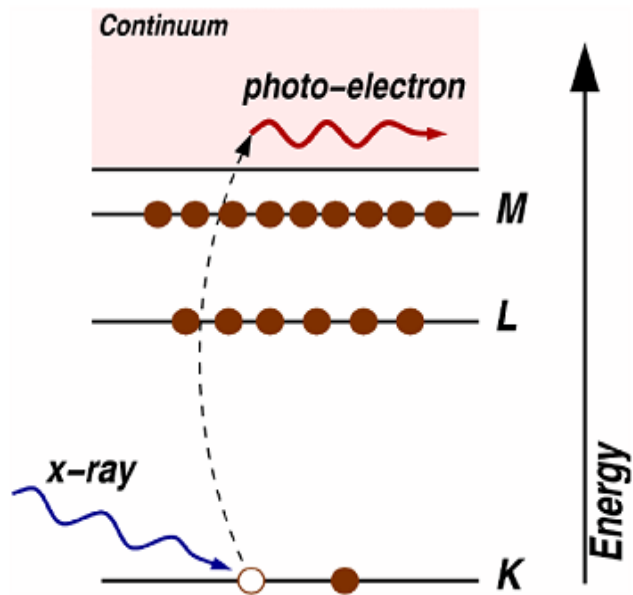


Fig. 2.2: Physics of X-ray Absorption (Newville, 2004)

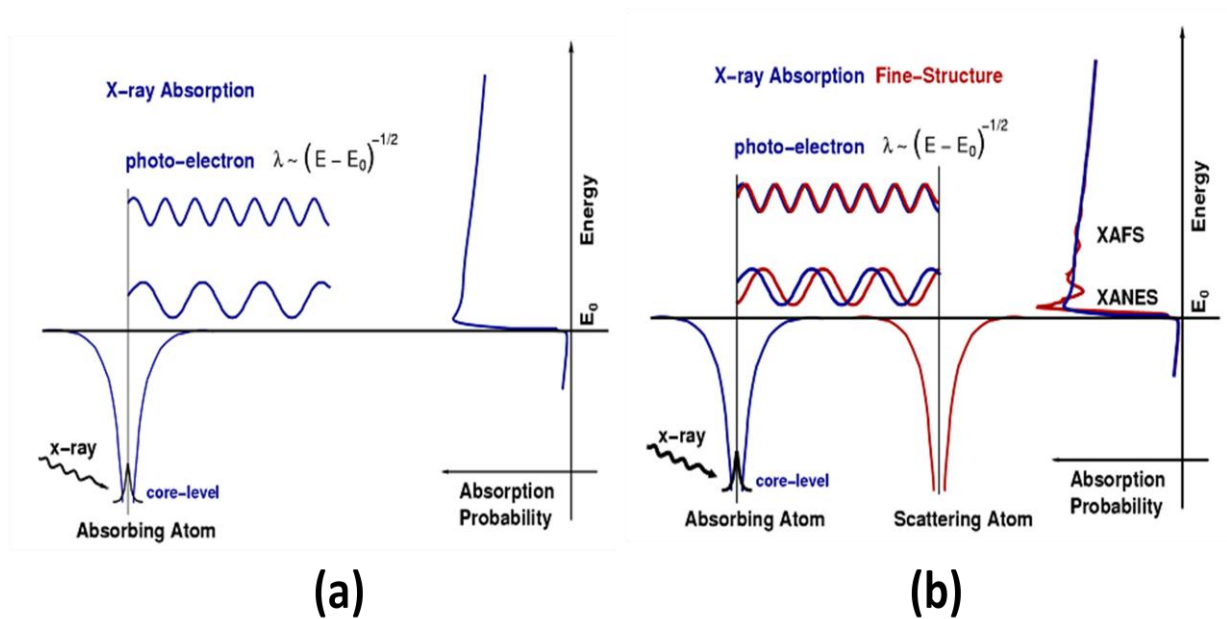


Fig. 2.3: (a) X-ray absorption by a free atom, (b) X-ray absorption in the presence of neighboring atoms (Newville, 2004)

Being electron wave scattering phenomenon, XAFS information is inherently local in nature and hence can be used for studying local-scale defects. Over the years, understanding of local-scale defects (for example, their role on electronic structure) has

gained importance, as long-range-order (LRO) could not adequately explain many of the phase transitions.<sup>47-52</sup> The other strengths of XAFS are (i) due to the “local” nature of information, crystalline samples are not required. This makes XAFS the unique structural tool for both crystalline and amorphous systems (e.g. disordered nanoparticles, metallic glass, soil, liquid)<sup>53-59</sup> which lack Long Range Order, and hence structural tools such as X-ray Diffraction are insufficient to decode the structure. (ii) Tunability: In a multi-component system, XAFS, being an element-specific probe, can extract site-resolved structural information.<sup>60-64</sup> This is useful to understand the exact role of each component in the scientific problem of interest. (iii) Since XAFS is not inherently surface sensitive, penetration depth can be controlled to carry out both bulk and surface measurements by changing the angle of incidence of x-rays on the sample. (iv) XAFS has ppm range detection limit, and hence can be applied to even very dilute dopants. (v) XAFS can be measured under extreme thermodynamic conditions – low temperature, high pressure, high temperature.

### 2.3 The XAFS Equation

XAFS is defined as:

$$\chi(E) = \frac{\mu(E) - \mu_0(E)}{\Delta\mu_0(E_0)} \quad (2.1)$$

where,  $\mu(E)$  is the measured absorption coefficient;  $\mu_0(E)$  is the slowly varying background absorption from isolated absorbing atom and other processes;  $\Delta\mu_0(E_0)$  is the measured jump in absorption coefficient at threshold energy  $E_0$ .

XAFS is an interference effect and depends on the wave-nature of the photo electron. Therefore it is convenient to think of XAFS in terms of the photo-electron wave

number rather than the X-ray energy. The XAFS oscillations are hence conventionally described *wrt* the photo-electron wave number,  $k$ .

$$k = \sqrt{\frac{2m(E - E_0)}{\hbar^2}}, \quad (2.2)$$

where  $m$ =electron mass,  $E = \hbar\omega$  is the energy of the absorbed x-ray photon.

X-ray absorption is a transition between two quantum states. The initial state contains an x-ray photon and a core-electron and no photo-electron. The final state contains no x-ray photon, a core-hole and a photo-electron. Therefore,  $\mu(E)$  can be described using Fermi's Golden Rule<sup>65</sup>:

$$\mu(E) \sim |\langle i | H | f \rangle|^2, \quad (2.3)$$

where,  $\langle i |$ : The initial state (x-ray photon + core electron). This is not altered by the neighboring atom.

$H$ : the interaction. In the dipole approximation,

$$H = e^{ikr} \approx 1. \quad (2.4)$$

$|f\rangle$ : The final state (core-hole + photo-electron). This is altered by the neighboring atom.

Hence the absorption is modulated.

Now,  $|f\rangle = |f_0\rangle + |\Delta f\rangle$ , i.e. sum of the bare atom  $|f_0\rangle$  and the effect of the neighboring atom  $|\Delta f\rangle$ .

Then, the bare atom absorption,

$$\mu_0 = |\langle i | H | f_0 \rangle|^2 \quad (2.5)$$

and the fine structure,

$$\chi(E) \propto |\langle i | H | \Delta f \rangle|^2. \quad (2.6)$$

$H$  represents the process of interchange of two energy and momentum states.

The absorption is proportional to the amplitude of the photo electron at the origin.

Consider an outgoing photo-electron described by a spherical wave number  $k$  ( $k = 2\pi/\lambda$ ;

$\lambda = h/p$ ) and amplitude  $A$ :

$$A \propto \frac{e^{ikr}}{r} \quad (2.7)$$

The neighboring atoms scatter this spherical wave into a new spherical wave. This backscattered wave is proportional to the amplitude of the incident wave and the backscatter type-dependent backscattering amplitude  $F(2k)$ , i.e.

$$F(2k) \frac{e^{ikr}}{r} \frac{e^{ik|r-r_i|}}{|r-r_i|}$$

The backscattered wave emanates from  $r$  and not from the point of origin of the outgoing spherical wave. However, it is the intensity of the backscattered wave at the origin ( $r \sim 0$ ) which is of interest to us. This is because the initial state is an s-state, which is non-zero close to the origin, therefore  $\langle i|H|\Delta f \rangle \neq 0$  only close to the origin. Amplitude of the backscattered wave at the origin is proportional to

$$F(2k) \frac{e^{i2kr}}{r^2}.$$

The factor  $2kr_i$  is the phase shift introduced by a wave of wave number  $k = 2\pi/\lambda$  in traveling distance  $2r_i$  from the origin and back from the backscatterer. However, since the electron is not traveling in constant potential, a phase shift  $\delta(k)$  must be incorporated to account for the varying potentials of the absorber and backscattering atoms.

$$\delta(k) = 2\delta_a(k) - l\pi + \delta_b(k), \quad (2.8)$$

where  $\delta_a(k)$  and  $\delta_b(k)$  denote the phase shifts due to absorber and backscatterer

respectively (Fig. 2.4);  $l=1$  for K-edge. [Note that  $\delta_a(k)$  has to be counted twice in the sum].

$$\text{Therefore, } \chi(k) \propto F(2k) \frac{e^{i[2kr+\delta(k)]}}{2r^2} = \frac{F(2k) \sin(2kr + \delta(k))}{r^2} \quad (2.9)$$

The backscattered wave modifies the absorption as it interferes with the outgoing wave, and this modification is, by definition, the EXAFS.

Since the absorber atom usually has more than one neighboring atom, the above equation must be summed over the scattering contributions from all neighboring atoms. In the single scattering approximation, the effect of many scatterers can be obtained simply by adding the effects of each scatterer, and the total EXAFS becomes

$$\chi(k) = K \sum_j \frac{F_j(2k) \sin(2kr_j + \delta_j(k))}{r_j^2} \quad (2.10)$$

where  $K$  is a constant of proportionality.

$$KF_j(2k) = \frac{m}{2\pi\hbar^2} f_j(2k) \quad (2.11)$$

In any coordination shell, all the atoms will not be exactly at the same distance because of thermal vibrations or structural disorder. Thus the contributions of these atoms will not all exactly be in phase. If this disorder is small, and has a Gaussian distribution about the average distance  $R_j$ , i.e. it has a probability of deviating from the average by

$$\left(2\pi\sigma_j^2\right)^{-1} \exp\left(-\frac{(r_j - R_j)^2}{2\pi\sigma_j^2}\right),$$

the de-phasing produced by it adds a factor  $N_j \exp(-2k^2\sigma_j^2)$  to the EXAFS expression instead of  $N_j$ , where  $N_j$  is the number of atoms of type  $j$  in the shell and  $\sigma_j$  is the RMS deviation from the average distance  $R_j$ . The EXAFS expression in equation 2.10 is modified as

$$\chi(k) = \frac{m}{2\pi\hbar^2} \sum_j \frac{f_j(2k)N_j \exp(-2k^2\sigma_j^2) \sin(2kr_j + \delta_j(k))}{r_j^2} \quad (2.12)$$

So far, this derivation has left out an important physical effect: the lifetime  $\tau_0$  of the photo-electronic states. This has two contributions: (i) the time taken for the core-hole to be filled by another electron and (ii) the lifetime of the photo-electron itself. These two lifetimes contribute to determine the finite lifetime of the excited state consisting of the photo electron together with the core-hole from which it came. The lifetime is important because in order for the backscattered wave to interfere with the outgoing wave, the two must be coherent, i.e. the phase difference between the two must be well defined. This depends on  $\lambda$ , the mean free path of the electron, which defines the distance upto which an electron can travel before being inelastically scattered.  $\lambda \sim 8-10\text{\AA}$ , which is responsible for the local nature of XAFS. Therefore, another exponential decay factor  $\exp(-2r_j/\lambda)$  is introduced into equation 2.12, which accounts for the inelastic losses suffered by the electron during the scattering process. The equation now becomes:

$$\chi(k) = \frac{m}{2\pi\hbar^2} \sum_j \frac{f_j(2k)N_j \exp(-2k^2\sigma_j^2) \exp(-\frac{2r_j}{\lambda}) \sin(2kr_j + \delta_j(k))}{r_j^2} \quad (2.13)$$

Further, an additional factor, called the amplitude reduction factor or  $S_0^2$ , is introduced, which accounts for relaxation of all other electrons in the absorber atom due to creation of the core-hole. It has element-specific constant value.<sup>66</sup> Usually,  $0.7 < S_0^2 < 1$ . The equation is then modified as:

$$\chi(k) = \frac{m}{2\pi\hbar^2} \sum_j \frac{S_0^2 f_j(2k)N_j \exp(-2k^2\sigma_j^2) \exp(-\frac{2r_j}{\lambda}) \sin(2kr_j + \delta_j(k))}{r_j^2} \quad (2.14)$$

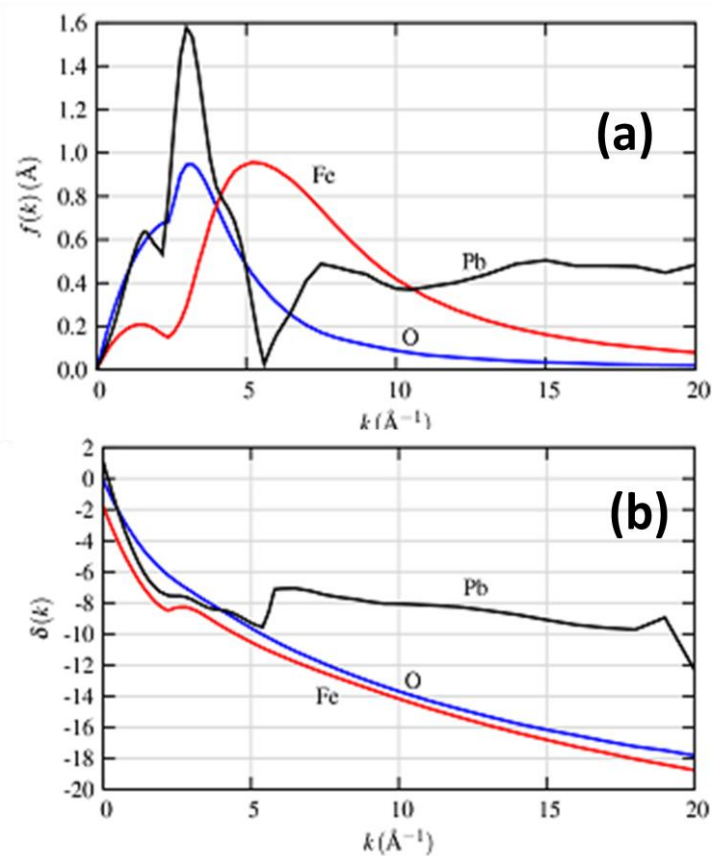


Fig. 2.4: Dependence of (a) scattering amplitude  $f(k)$  and (b) phase shift  $\delta(k)$  on scatterer type (Newville, 2004)

The XAFS equation is the superimposed result of the structural information from different atoms at different distances. From equation 2.14, it is clear that the period of XAFS oscillations is given by  $r_j$ , the radial coordinates of the neighboring atoms, and the amplitude is proportional to  $N_j$ , the coordination number of the neighboring atoms. To decouple this information, the oscillations are Fourier transformed to yield a radial distribution function (corrected phase shifts) of atoms. The positions of the peaks in the distribution correspond to the different radial distances from the absorbing atom at which the surrounding atoms are located and the amplitudes of the peaks correspond to the number of these atoms. Each of these peaks is then fitted using the structural parameters (coordination number, atomic type, bond length, Debye Waller Factor) as variables. The

theoretical accuracy with which these parameters can be determined are  $r = \pm 0.01 \text{ \AA}$ ,  $\sigma^2 = 0.002 \text{ \AA}^2$ ,  $N = \pm 1$ ,  $Z = \pm 5$ .

The following is the summary of approximations used while deriving the XAFS equation:

1. Dipole Approximation: The Electric Field over the electromagnetic wave is assumed to be constant over the dimensions of the K-shell, so that the interaction Hamiltonian,

$$H = e^{ikr} \approx 1. \quad (2.15)$$

This selection rule ( $\Delta l = \pm 1$ ) implies that (a) if the initial core has s-symmetry ( $l=0$ , edges K and  $L_I$ ), the final state has p symmetry ( $l=1$ ); (b) if the initial core-state has p symmetry ( $l=1$ , edges  $L_{II}$  and  $L_{III}$ ), the final state can have s or d symmetry ( $l=0$  or  $l=2$  respectively). However, sometimes, dipole-forbidden transitions become 'allowed' due to hybridization between states, giving non-negligible contributions to XAFS.

2. Muffin-tin approximation: The muffin-tin potential is a spherical scattering potential centered on each atom, with a constant value of potential in the interstitial region between the atoms. In the EXAFS domain, the kinetic energy of the photo-electron is large; therefore the electron is less sensitive to details of the potential at the outer edges of the atom and in the region between the atoms. As a result, the electron is mainly scattered by the inner parts of the atomic potential and it moves more-or-less freely in the average potential within the flat interstitial region. Therefore, the muffin-tin potential approximation works well in the EXAFS regime. However, the details of the potential are much more important for XANES calculations where the photoelectron has low kinetic energy.

3. Plane wave approximation: The plane wave approximation is valid if the effective size of the atom in backscattering is small compared with the distance between the atom and the center atom. At low  $k$ , this is not case, because the effective atomic size is about the same as inter-atomic distance. As the  $k$  of the photoelectron increases, the effective size of the atom decreases as the photoelectron penetrates deeper into the atom before scattering. The electron will scatter significantly only when the spatial variation of the atomic potential has a significant fractional change in the distance of  $1/k$ . At high  $k$  the diminishing effective size of the backscattering atom makes the small-atom approximation satisfactory.

The effect of the breakdown of the small-atom approximation on the phase of EXAFS can be approximately compensated for by a shift of  $E_0$ . Here  $E_0$  is the

binding energy of the photoelectron and is related to  $k$ :  $k = \sqrt{\frac{2m(E - E_0)}{\hbar^2}}$ .

However,  $E_0$  shifts cannot correct for amplitude error introduced by the small atom approximation. Eliminating the small-atom approximation makes EXAFS less convenient because  $f(2k)$  and  $\delta(k)$  then depend on  $r_j$  in addition to  $k$ , and their tabulation would become prohibitive because of the additional parameter of  $r_j$ .

4. Quasi-independent particle approximation: While deriving the XAFS equation, we have initially ignored the fact that the remaining (N-1) states will no longer have the same wave function as the core-electron is rejected and correspondingly a hole is created. This incomplete overlap reduces the measured XAFS amplitudes. To compensate for this, the term  $S_0^2$  is introduced in the equation.
5. Single scattering approximation: The derivation of XAFS equation was based only on single scattering process of the photo-electron. Multiple scattering effects, which are important for XANES and also in the EXAFS regime in certain cases,

have been ignored. The multiple scattering effects are discussed in the following section.

6. The equation was derived for 1s initial state (K-edge) for which there is only one possible final state (p-state). For a p or d initial state (L or M edge), there will be two possible final states and hence the equation will have a more complicated angular dependence.

## 2.4 Multiple Scattering

As mentioned above, the derivation of the EXAFS equation (2.14) was based on the single scattering approximation – that the outgoing wave is backscattered from the surrounding atom only once before combining with the unscattered wave. This approximation is valid only so long as the scattering is small. For further scatterings such as scattering from one neighbor to the next before combining with the unscattered wave, the equation must be modified further.

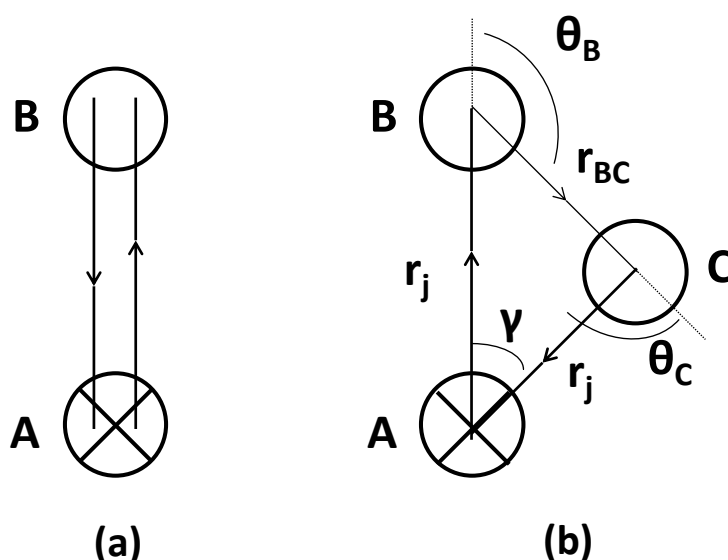


Fig. 2.5: (a) Single Scattering path for photo electron, (b) Double scattering path for photo electron

Consider the three atom systems shown in Fig. 2.5, with atom A being excited by absorbing the x-ray photon. We compare two processes. Fig. 2.5 (a) is the single scattering case wherein the photo-electron is back scattered from atom B and interferes with the outgoing state at atom A. Fig. 2.5(b) is the double scattering case wherein the photoelectron scatters from atom B and then atom C before returning to atom A and interfering with the outgoing state. This double scattering contribution produces a backscattered wave of the form

$$\frac{F(\theta_B)F(\theta_C)\exp i[k(2r_j + r_{BC}) + \delta_m(k) - \pi/2]}{kr_j^2 r_{BC}} \cos\gamma \quad (2.16)$$

where  $\delta_m(k) = 2\delta_1 + \beta_B + \beta_C$ ,  $F(\theta_B)$  is the amplitude of scattering from atom B through an angle  $\theta_B$ , and  $\beta_B$  is the phase introduced by that scattering.  $\gamma$  is the angle between the first and last scattering paths.  $\cos\gamma$  measures the overlap of the p state of the final incoming electron with the p-state excited by the x-ray. A Fourier Transform of equation 2.16 will peak at the larger distance  $R \cong \frac{r_j + r_{BC}}{2}$ , neglecting the shift caused by the k dependence of the phase  $\delta_m$ . The magnitude of the backscattering amplitude is  $F/r_{BC}$  times that of single scattering. For  $\theta_B, \theta_C > 40^\circ$ ,  $F(\theta)/r_{BC} \cong F(\pi)/r_{BC}$ , which is small for  $r_{BC} \geq 2 \text{ \AA}$ . However, for  $\theta \cong 0^\circ$ ,  $F(0)$  peaks and becomes much larger (see Fig. 2.4(a)).  $F(\theta)/r_{BC} \cong 1$  and double scattering becomes important. This forward scattering configuration is called the focusing or shadowing effect and is the only case where double scattering is important relative to single scattering in the same shell.

Forward multiple scattering has been used to determine atomic configurations where three atoms are aligned or almost aligned.<sup>67</sup> It has also been used to determine unit cell tilt angles in several cases.<sup>43,55,68</sup>

It is to be noted that all multiple scatterings peak in the Fourier Transform only at distances larger than that of the single scattering first neighbor. Thus the first neighbor peak in the Fourier Transform has rigorously no multiple scattering contributions.

## 2.5 Brief overview of XANES

XANES is a region of x-ray absorption spectrum within 30eV of the absorption edge. Although the basic physics of XANES is same as that of EXAFS, the low kinetic energy of the photo-electron in the XANES region results in a different phenomenon. Since the De-Broglie wavelength of the photo-electron is very large ( $\sim 100\text{\AA}$ ) in the XANES region, it spills over several bondlengths; therefore the local structural resolution is lost. However, due to low kinetic energy, the photo-electron wave becomes very sensitive to the chemical potential so that it can recognize chemical state of the atom. Because of low kinetic energy, it is susceptible to multiple scattering so that it can detect site symmetry (tetrahedral vs. octahedral). Hence, important information such as charge transfer/oxidation state/site symmetry can be obtained from XANES

Fig. 2.6 shows a typical XANES spectrum. It can be divided into the following regions:

- (i) Pre-edge refers to the region just before the edge step. Pre-edge features are caused by electronic transitions to empty bound states, the transition probability being governed by dipole selection rules. The pre-edge contains information pertaining to local geometry around absorbing atom and shows strong dependence on oxidation state and bonding characteristics (chemical shift) of absorbing atom.
- (ii) Edge refers to the absorption edge. It defines the ionization threshold for transition to continuum states. It shows strong oxidation state dependence as well.

(iii) Whiteline refers to a sharp peak in the spectrum just above the edge. Its intensity is proportional to the density of unoccupied states and it is strongly dependent on the oxidation state as well.

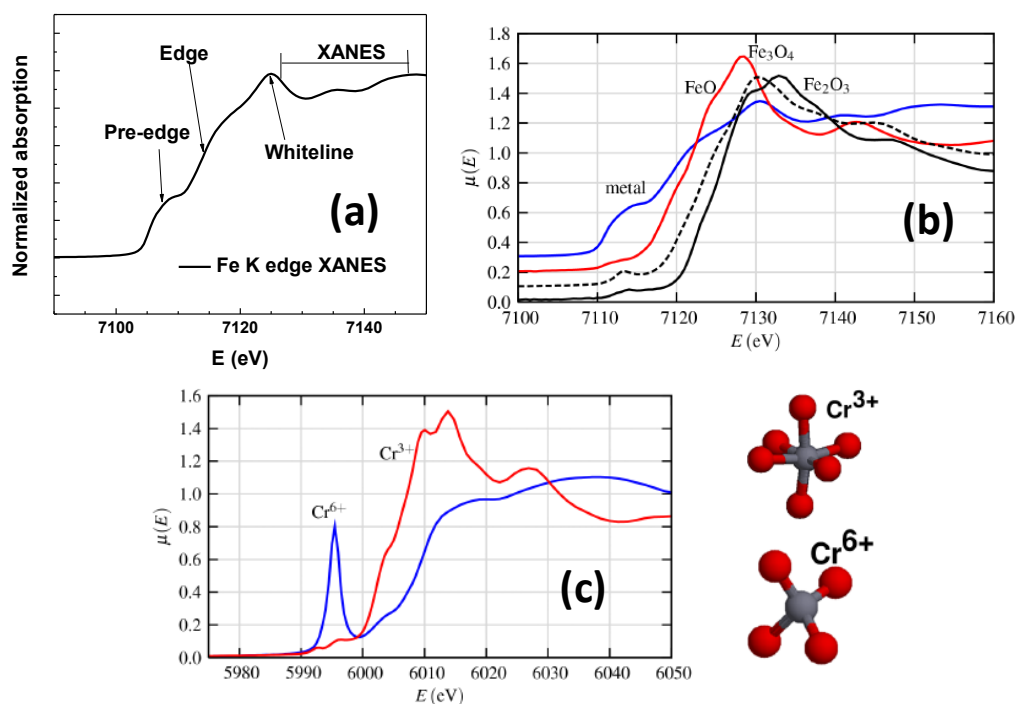


Fig. 2.6: (a) Typical XANES spectrum. XANES can be used to qualitatively detect (b) oxidation state, (c) site symmetry. (Newville, 2004)

(iv) XANES features arise due to multiple scattering resonances of photo electrons ejected at low kinetic energy. They contain information on inter-atomic distances and bond angles.

A lot of chemical information is obtainable from XANES, particularly the valence (very difficult to experimentally determine in a non-destructive way) state of the absorbing atom and its coordination environment. Since the edge position and shape are sensitive to formal valence state, ligand type, and coordination environment, the same are reflected in the edge features.

**2.5.1 Oxidation State:** Change in oxidation state is reflected as: (i) shift in absorption edge position (positive shift = higher oxidation state). Increase in oxidation state is equivalent to an increase in the attractive potential of the nucleus following loss of an electron. (ii) change in “whiteline” intensity. Whiteline intensity is proportional to the density of unoccupied final states, which is related to the oxidation state of the sample. Higher the oxidation state, sharper is the whiteline intensity. The determination of exact oxidation state from whiteline intensity is complicated by the effect of coordination geometry on the transition probabilities. But, the systematic change in whiteline intensity can be used to monitor relative charge-transfer related phenomena as a function of dopant concentration for eg. in intermetallics or the time evolution of species during a chemical reaction by time-resolved in-situ experiments. This leads to important applications of XANES in two important fields – environmental science and catalysis.

**2.5.2 Site symmetry:** Coordination geometry of nearest neighbors around the absorbing atom lays its signature in XANES through orbital hybridization of unoccupied states. Although X-ray absorption is dominated by dipole transition rule ( $l=\pm 1$ ), weak pre-edge features result if there is hybridization between orbitals of suitable symmetry. For eg. in K-edge XANES, although the transition is from  $1s \rightarrow p$  state, there could be pre-edge features resulting from p-d mixing. For octahedral symmetry, no p-d mixing is allowed and only a weak pre-edge feature may be present from quadrupole transition. For tetrahedral symmetry, pre-edge feature has highest intensity. Distorted octahedral also result in pre-edge features. Therefore, pre-edge intensity is a qualitative mark of distortion from octahedral symmetry.

## **2.6 Strengths and Limitations of XAFS**

Just like every other technique, XAFS has its own advantages and limitations. The main advantage is the “local” nature of XAFS information, making it possible to

determine accurate structures for non-crystalline samples. Several important length scales in science, e.g. coherence length of charge carriers in high  $T_c$  superconductors, length scales of magnetic interactions, chemical interactions, interface binding, fall in the “local” structure regime. This local structure is at times significantly different from the average Long Range Order detected by conventional structural techniques like diffraction. Local structural information, for e.g. nanoscale phase separation, local structural inhomogeneities, dopant induced disorder, can provide the key to understanding several material properties and novel phenomena like Metal-insulator transition, persistence of superconductivity beyond crystallographic transition, switching phenomena, luminescence stability, glass forming ability etc..<sup>49,51,53-69</sup>

In ideal circumstances, EXAFS data can be analyzed to determine the absorber-scatterer distance with an accuracy of at least  $\sim 0.02 \text{ \AA}$ . Coordination numbers can be determined with an accuracy of  $\sim 25\%$  and scatterer identity can typically be defined to the nearest row of the periodic table.

XANES analysis provides oxidation state and spin-state information that can be difficult or sometimes even impossible to extract from crystallographic measurements. In comparison with other spectroscopic methods, XAFS has the decided advantage that it is always detectable, without the need for specific spin states or isotopic substitution, and that it is element specific.

There are, of course, some limitations of EXAFS. Firstly, it provides only limited chemical resolution - scattering atoms that differ by  $\Delta Z \leq 5$  (e.g. C, O, N, and F) typically cannot be resolved. Secondly, the finite  $k$  range of the EXAFS spectrum limits the bond-length resolution of the method. Two scattering shells can only be resolved if they differ sufficiently in frequency to cause a detectable change in the EXAFS amplitude. Finally, it only gives the bond distances and not the actual coordinates of the neighboring atoms.